

CLC-3 deficiency leads to phenotypes similar to human neuronal ceroid lipofuscinosis

Momono Yoshikawa¹, Shinichi Uchida^{1,*}, Junji Ezaki², Tatemitsu Rai¹, Atsushi Hayama¹, Katsuki Kobayashi¹, Yujiro Kida¹, Masaki Noda³, Masato Koike⁴, Yasuo Uchiyama⁴, Fumiaki Marumo¹, Eiki Kominami² and Sei Sasaki¹

¹Homeostasis Medicine and Nephrology, Graduate School, Tokyo Medical and Dental University, 1-5-45 Yushima Bunkyo Tokyo 113-8519, Japan

²Department of Biochemistry, Juntendo University School of Medicine, 2-1-1 Hongo Bunkyo Tokyo 113-8421, Japan

³Department of Molecular Pharmacology, Medical Research Institute, Tokyo Medical and Dental University, 2-3-10 Kanda-surugadai Chiyoda Tokyo 101-0062, Japan

⁴Department of Cell Biology and Neurosciences, Osaka University Graduate School of Medicine, 2-2 Yamadaoka Suita Osaka 565-0871, Japan

Abstract

Background: CLC-3 is a member of the CLC chloride channel family and is widely expressed in mammalian tissues. To determine the physiological role of CLC-3, we generated CLC-3-deficient mice (*Clcn3*^{-/-}) by targeted gene disruption.

Results: Together with developmental retardation and higher mortality, the *Clcn3*^{-/-} mice showed neurological manifestations such as blindness, motor coordination deficit, and spontaneous hyperlocomotion. In histological analysis, the *Clcn3*^{-/-} mice showed a pattern of progressive degeneration of the retina, hippocampus and ileal mucosa, which resembled the phenotype observed in cathepsin D knockout mice. The defect of cathepsin D results in

a lysosomal accumulation of ceroid lipofuscin containing the mitochondrial F1F0 ATPase subunit c. In immunohistochemistry and Western blot analysis, we found that the subunit c was heavily accumulated in the lysosome of *Clcn3*^{-/-} mice. Furthermore, we detected an elevation in the endosomal pH of the *Clcn3*^{-/-} mice.

Conclusions: These results indicated that the neurodegeneration observed in the *Clcn3*^{-/-} mice was caused by an abnormality in the machinery which degrades the cellular protein and was associated with the phenotype of neuronal ceroid lipofuscinosis (NCL). The elevated endosomal pH could be an important factor in the pathogenesis of NCL.

Introduction

In mammals, the CLC chloride channel family consists of nine known members. The detection of inherited diseases that results from mutations in these genes and analyses of knockout mouse models are beginning to highlight the critical importance of the CLCs in biological processes. Mutations in the *CLCN1* gene lead to myotonia congenita, a disease characterized by disturbed muscle relaxation (Koch *et al.* 1992). Mutations in the *CLCNKB* gene cause Bartter's syndrome, a disease of renal salt wasting (Simon *et al.* 1997). Disruption of the *Clnk1* gene in mice (the homologue of human *CLCNKA*) leads to nephrogenic diabetes insipidus, a disease

caused by impairment of the countercurrent system (Matsumura *et al.* 1999). These phenotypes suggest that these chloride channels reside in the plasma membrane and mediate transepithelial chloride transport. On the other hand, mutations of CLC-5 lead to Dent's disease, a disorder characterized by the urinary loss of low-molecular-weight proteins, phosphate and calcium, and often lead to kidney stones (Günther *et al.* 1998). CLC-5 has been identified as an intracellular chloride channel co-localized with H⁺-ATPase in endosomes of the proximal tubules in the kidney (Günther *et al.* 1998; Sakamoto *et al.* 1999) and it has been shown to play a role in endocytosis (Piwon *et al.* 2000). While these findings suggest that CLC-5 provides a chloride shunt pathway for the efficient acidification of endosomes, this has not been confirmed by direct evidence. Considering the structural similarity between CLC-3 and CLC-5, the

Communicated by: Shoichiro Tsukita

*Correspondence: E-mail: suchida.kid@tmd.ac.jp

former may play a similar role to the latter in other tissues and cells. Recently, Stobrawa and colleagues reported that the disruption of *Cln3* leads to a severe postnatal degeneration of the retina and hippocampus (Stobrawa *et al.* 2001). However, it is still unclear how the disruption of *Cln3* leads to neurodegeneration.

To gain more insight into this pathogenesis, we generated and analysed the *Cln3*^{-/-} mice. We found that the neuronal abnormalities in the *Cln3*^{-/-} mice closely matched those in cathepsin D knockout mice (Saftig *et al.* 1995; Koike *et al.* 2000) and met the criteria for neuronal ceroid lipofuscinosis (NCL).

Results

Targeted disruption of the mouse *Cln3* gene

We disrupted the *Cln3* locus in mice by homologous recombination using a replacement vector with positive

(neo) and negative (TK) selection markers (Fig. 1A). This deleted exons 5 and 6 encoding transmembrane segments D2–D4 of the CLC-3 protein, an important region for ion permeation (Fahlke *et al.* 1997). Two recombinant ES cells were isolated and confirmed to be *Cln3*^{+/-}. These two clones generated five chimeras, four of which transmitted the mutant allele to their offspring. We subsequently intercrossed these heterozygous mice and yielded wild-type, heterozygous and homozygous progeny as determined by Southern blot analysis (Fig. 1B).

CLC-3 protein analysis

The absence of the CLC-3 protein was verified by Western blot analysis of protein fractions from brain tissues. We used a commercially available anti-CLC-3 antibody, which was recently shown not to cross-react with the closely related CLC-4 and CLC-5 proteins (Schmieder

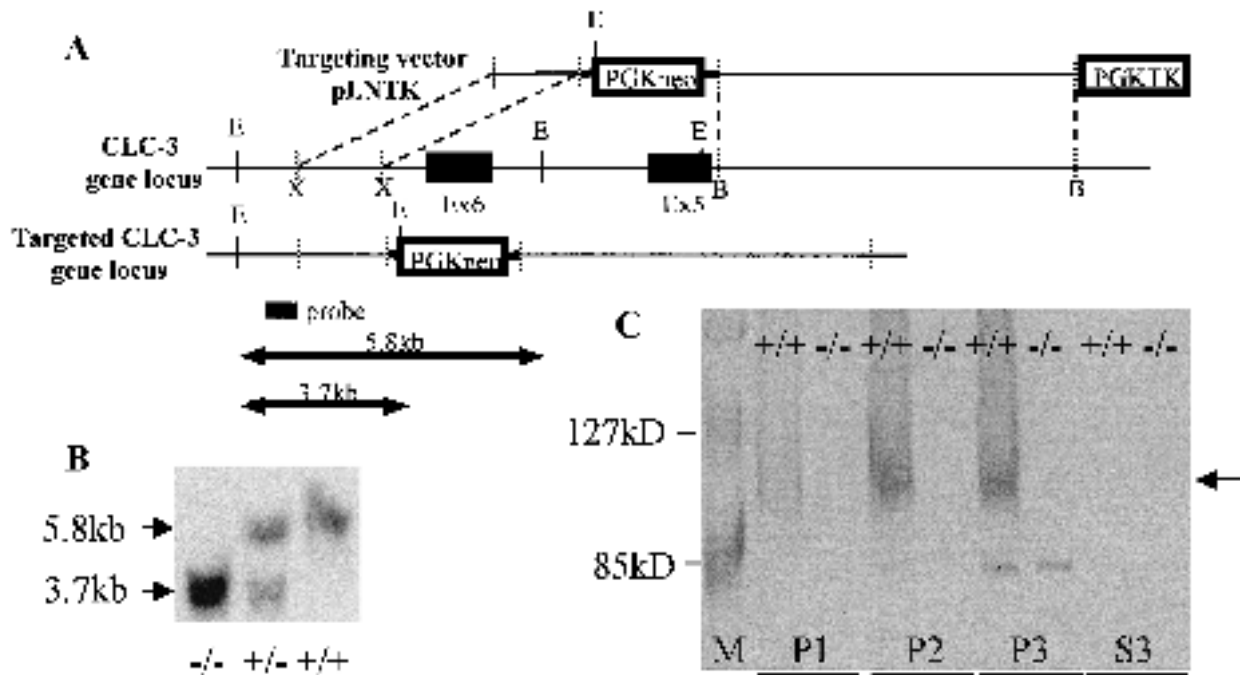


Figure 1 Generation of *Cln3*^{-/-} mice. (A) Diagram of the *Cln3* genomic locus, the targeting vector, and the predicted targeted allele. The exons are depicted as filled boxes. The 5' external probe used to detect the targeted allele is indicated under the diagram. The expected sizes of the *Eco*RI fragments that hybridize with the probe are indicated. PGKneo, neomycin transferase gene linked to the phosphoglycerate kinase (PGK) promoter; PGKTK, thymidine kinase gene derived from herpes simplex virus linked to PGK promoter. Both PGKneo and PGKTK were placed in a reverse orientation relative to *Cln3* transcription. E, *Eco*RI; X, *Xba*I; B, *Bam*HI. B, Southern blot analysis of genomic DNA extracted from mouse tails. DNA digested with *Eco*RI was electrophoresed, blotted, and hybridized with a probe. A 5.8 kb fragment from the wild-type allele and a 3.7 kb fragment from the mutant allele were detected. (C) A Western blot analysis of protein fractions from brain tissues immunoprobed with a C-terminal polyclonal antibody. This antibody recognized a CLC-3 band at 110–120 kDa and also a nonspecific band at 82 kDa. The molecular weight marker was loaded in lane M as a size standard. The CLC-3 protein (arrow) is absent in the *Cln3*^{-/-} mouse. P1, crude nuclear pellet (47 000 g pellet); P2, crude synaptosomes (120 000 g pellet); P3, crude synaptic vesicles (260 000 g pellet); S3, 260 000 g supernatant.

et al. 2001). In our Western blot analysis, this antibody recognized a ≈ 110 kDa smeary band in the synaptosomes (P2 in Fig. 1C) and in the synaptic vesicles (P3 in Fig. 1C) of the *Clcn3*^{+/+} mice, but no such band was found in the *Clcn3*^{-/-} mice. These results proved the absence of the CLC-3 protein in the *Clcn3*^{-/-} mice.

Skeletal abnormality, developmental retardation and higher mortality

The *Clcn3*^{-/-} mice were smaller than their normal littermates soon after birth. At 6 weeks the average body weight of *Clcn3*^{-/-} male mice was 18.1 ± 1.1 g ($n = 7$), or $\approx 25\%$ lower than that of their normal littermates (24.0 ± 0.9 g, $n = 9$). In an evaluation of their skeletal system by X-ray, they showed kyphoscoliosis (data not shown). The *Clcn3*^{-/-} mice also showed a higher mortality during the 3–4 weeks after weaning (33/116 in *Clcn3*^{-/-} and 1/198 in *Clcn3*^{+/+}). The mice that died were especially small, and necrosis of the whole small intestine was observed in all of their autopsies (Fig. 2A).

Neurological manifestations

Since CLC-3 was abundantly expressed in almost all regions in the brain, we performed a systemic analysis of gross neurological functions. The visible version of the water maze test suggested that the *Clcn3*^{-/-} mice were blind. While their muscle power was equal to that of weight-matched wild-type mice, we observed a performance deficit on the hanging wire test (Sango *et al.* 1996) (57.7 ± 2.0 s in *Clcn3*^{+/+}, $n = 12$; 28.4 ± 7.4 s, *Clcn3*^{-/-}, $n = 10$; $P < 0.01$, ANOVA). In the rotarod test, the *Clcn3*^{-/-} mice performed significantly worse than their littermate controls (29.5 ± 3.5 s in *Clcn3*^{+/+}, $n = 12$; 7.2 ± 1.6 s in *Clcn3*^{-/-}, $n = 10$, $P < 0.001$, ANOVA). We analysed the locomotor behaviour of the *Clcn3*^{-/-} mice in an open field and found that they spontaneously entered the hyperlocomotion phase at night (data not shown).

Selective degeneration of ileal mucosa, retina and hippocampus

We compared the gross morphology and histology of major organs between *Clcn3*^{+/+} and *Clcn3*^{-/-} mice at two months of age. Sagittal sections of brain revealed that the lateral ventricular system was enlarged to fill the void left by the atrophic hippocampus. At higher magnifications, we found a reduction in the density of pyramidal cells in the hippocampus in the *Clcn3*^{-/-} mice (Fig. 2B). The ileal mucosa was focally lost, even in the *Clcn3*^{-/-} mice (Fig. 2B) that were not dying. In the retina, the outer and inner

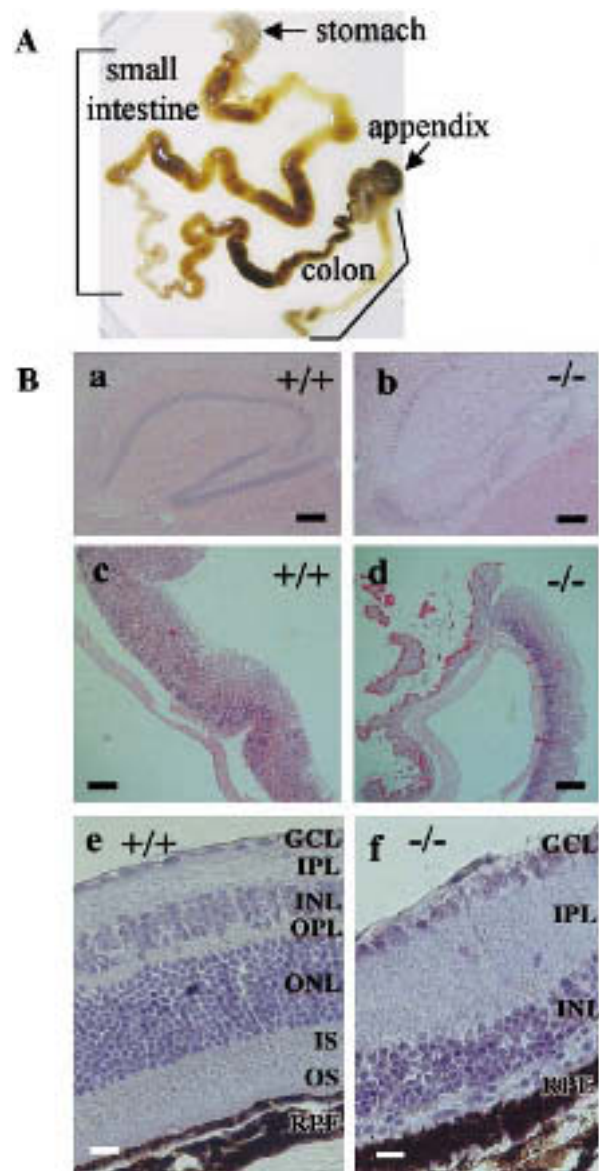


Figure 2 Selective degeneration of ileal mucosa, retina and hippocampus in *Clcn3*^{-/-} mice. (A) Macroscopic digestive tract phenotype in *Clcn3*^{-/-} mouse. Haemorrhagic-necrotic appearance of almost the entire small intestine was seen in the autopsy of this *Clcn3*^{-/-} mouse. (B) H&E-stained sections (5 μ m) of cerebrum, ileum, and eye in 2-month-old *Clcn3*^{+/+} (a, c, e) and *Clcn3*^{-/-} (b, d, f) mice. The *Clcn3*^{-/-} mouse showed a reduction in pyramidal cell density in the hippocampus (b). The *Clcn3*^{-/-} mouse showed a focal atrophy of the ileal mucosa (d), that was somewhat less severe than that in the mortal mouse shown in (A). In the retina, photoreceptors in ONL were completely lost in *Clcn3*^{-/-} mouse (f). RPE, retinal pigment epithelium; OS, photoreceptor outer segment; IS, photoreceptor inner segment; ONL, outer nuclear layer; OPL, outer plexiform layer; INL, inner nuclear layer; IPL, inner plexiform layer; GCL, ganglion cell layer. Scale bars indicate 50 μ m (a, b), 100 μ m (c, d), and 10 μ m (e, f).

segments and the outer nuclear layer were completely absent (Fig. 2B), indicating photoreceptor degeneration.

Lysosomal accumulation of subunit c of mitochondrial F1F0ATPase

During our morphological examination of the *Cln3*^{-/-} mice, we noticed that our findings resembled the phenotype observed in cathepsin D knockout mice (Saftig *et al.* 1995; Koike *et al.* 2000). Recently, cathepsin D knockout mice were shown to have the characteristics of NCL (Koike *et al.* 2000), which showed massive lysosomal storage with autofluorescent lipopigment. To test whether the neuronal degeneration in the *Cln3*^{-/-} mice resulted from a similar mechanism, we examined the morphological, immunohistochemical and biochemical features of the *Cln3*^{-/-} mice. Electron microscopy showed abundant lysosome-like structures in the perikarya of pyramidal neurones in the hippocampus (Fig. 3a). These structures resembled lipofuscin granules and exhibited a similar irregular profile and heterogeneous electron-density. In the astrocytes, we observed autolysosome- or autophagosome-like bodies encircled by a single layer of a limiting membrane and containing numerous membranous structures (Fig. 3b). In many types of NCLs and cathepsin D knockout mice, subunit c of mitochondrial F1F0 ATPase is stored in lysosomes. An immunohistochemical analysis performed on *Cln3*^{-/-} mice at the age of 6 weeks, just before the hippocampus was completely degenerated, showed a clear positive staining of subunit c in neuronal cells in the olfactory bulb, hippocampus, cerebellum and cerebral cortex (Fig. 4), i.e. in all of the organs where CLC-3 mRNA was abundantly expressed (Kawasaki *et al.* 1994).

Next, we biochemically examined the lysosomal localization of stored subunit c in brains and livers. Figure 5 summarizes the reactivities of the antibodies against various mitochondrial proteins (subunit c, β of ATP synthase, and subunit IV of cytochrome oxidase) and lysosomal proteinases (cathepsin D and TPP-I). A significant amount of subunit c was detected in the lysosomal fractions in the *Cln3*^{-/-} mice, whereas subunit c was found almost exclusively in the mitochondrial fractions in the *Cln3*^{+/+} mice. At the age of 27 weeks, the lysosomal accumulation of subunit c was slightly increased in the liver, but somewhat decreased in the brain, reflecting a loss of damaged cells. The β subunit of ATP synthase and cytochrome oxidase subunit IV were only detected in mitochondrial fractions of *Cln3*^{-/-} and *Cln3*^{+/+} mice. Finally, we examined whether the levels of TPP-I and cathepsin D, two lysosomal proteases which are known to be involved in the lysosomal degra-

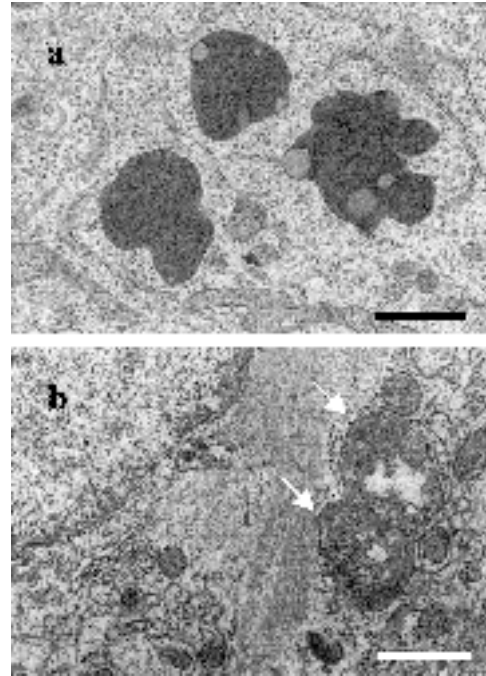


Figure 3 Electron micrographs of neuronal and glial cells in the hippocampus of a *Cln3*^{-/-} mouse brain. (a) A neurone having a large round nucleus possessed various organelles that are normally distributed in the perikarya. Lysosome-like structures with an irregular form and heterogeneous electron density were also seen in abundance in the perikarya, mimicking the appearance of lipofuscin granules. (b) An astrocyte containing bundles of intermediate filaments in the cytoplasm possessed an autolysosome- or autophagosome-like body encircled by a single layer of the limiting membrane and containing numerous membranous structures (arrow). Scale bars = 1 μ m.

dation of subunit c (Ezaki *et al.* 1999; Koike *et al.* 2000), are processed into the mature active forms in *Cln3*^{-/-} mice. As shown in Fig. 5, the mature form of TPP-I (46 kDa) and the single-chain mature form of cathepsin D were observed in lysosomal fractions of the brain and liver of *Cln3*^{-/-} mice, whereas the TPP-I precursor form (67 kDa) and procathepsin D (53 kDa) were undetectable. These data suggested that the precursor forms of TPP-I and cathepsin D were effectively processed into the enzymatically active mature forms in the brains and livers of both the *Cln3*^{-/-} mice and control mice.

Impaired acidification of endosomal compartments

To gain more insight into the pathogenesis of NCL in the *Cln3*^{-/-} mice, we measured the intraluminal pH in the CLC-3-containing intracellular vesicles in the liver, since the NCL phenotype was observed in the liver (Fig. 5)

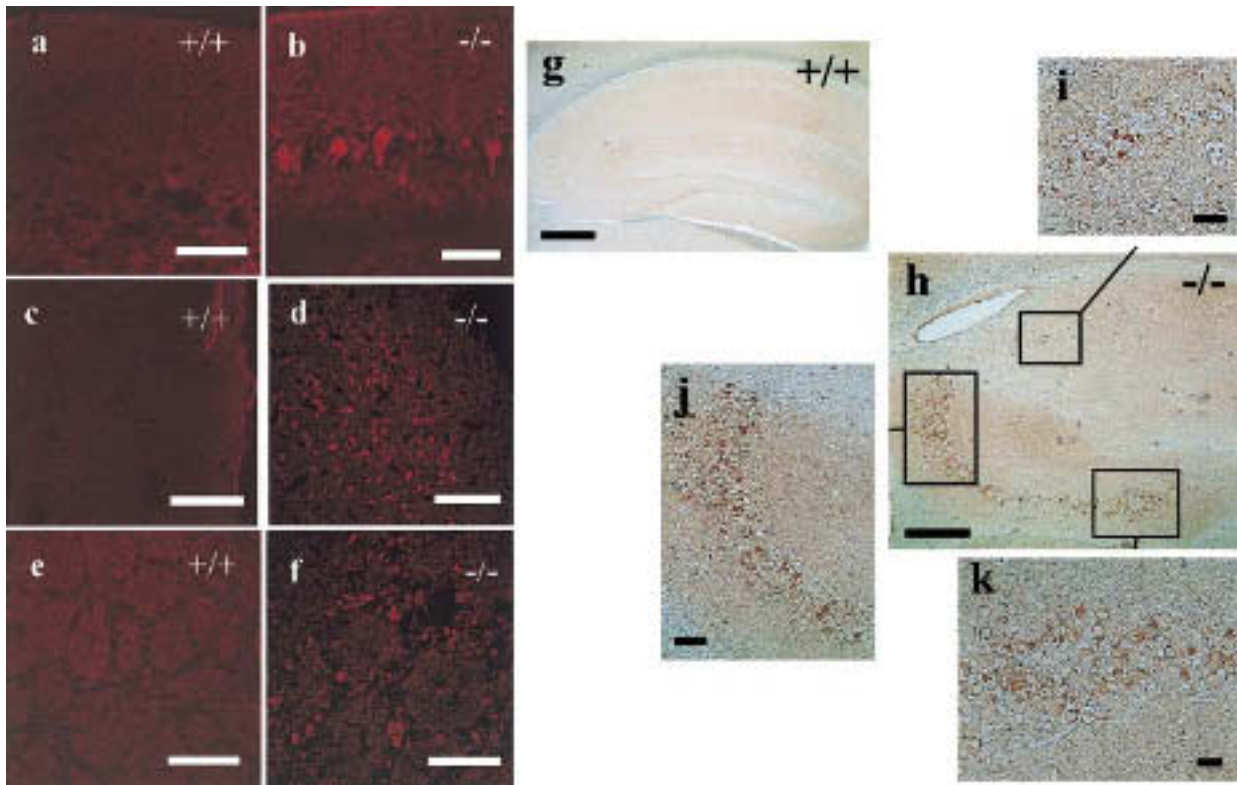


Figure 4 Immunohistochemical demonstration of subunit c of mitochondrial F1F0 ATPase in *Clcn3*^{-/-} mouse brain. Immunostaining for subunit c of mitochondrial F1F0 ATPase in wild-type mice and *Clcn3*^{-/-} mouse at 6 weeks of age. Subunit c was not stained in the *Clcn3*^{+/+} mouse brain (a, c, e, g). In the *Clcn3*^{-/-} mouse brain, subunit c was stained in the Purkinje cell layer of the cerebellum (b) and pyramidal cells of the cerebral cortex (d), olfactory bulb (f) and hippocampus (h), all the sites where CLC-3 mRNA was abundantly expressed. Scale bars = 50 μ m (a–h), and 10 μ m (i–k).

and intravesicular pH measurement in the brain cells was not successful. In a Western blot analysis, CLC-3 was found to be concentrated in the P3 fraction (100 000 g pellet) containing endosomes, and not in the P2 fraction (10 000 g pellet) containing lysosomes and mitochondria (data not shown). We prepared a FITC-dextran-loaded P3 fraction from the wild-type and *Clcn3*^{-/-} mice, and compared their steady-state intravesicular pH values in the presence of ATP. The mean steady-state pH in the vesicles was 6.37 ± 0.04 for the *Clcn3*^{+/+} mice ($n = 4$) and 6.76 ± 0.09 for the *Clcn3*^{-/-} mice ($n = 3$). The difference between groups was statistically significant ($P < 0.01$, unpaired *t*-test), confirming that CLC-3 is involved in the regulation of intravesicular pH homeostasis.

Discussion

While we were preparing this manuscript, Stobrawa *et al.* published a separate report on the generation of *Clcn3*^{-/-} mice (Stobrawa *et al.* 2001). Growth defects,

higher mortality and hyperlocomotion were common findings. They also demonstrated a postnatal degeneration of the retina and hippocampus, but they did not mention a degeneration of the ileal mucosa and they did not describe the pathogenesis of neuronal degeneration. A morphological examination of the *Clcn3*^{-/-} mice showed that they resembled cathepsin D knockout mice in terms of retinal atrophy, neuronal degeneration, and focal, sometimes total, atrophy of the ileal mucosa (Saftig *et al.* 1995; Koike *et al.* 2000). Recently, Koike *et al.* reported that cathepsin D knockout mice had characteristics of NCL (Koike *et al.* 2000).

NCLs are a group of inherited lysosomal storage diseases characterized by progressive blindness, psychomotor retardation and premature death (Goebel 1995; Goebel & Sharp 1998; Dawson & Cho 2000). Pathologically, autofluorescent lipopigment accumulates in lysosome-derived organelles in neurones and cells in other organs. Recent studies have shown that the various forms of

NCLs result from mutations in at least eight genes. These include the soluble lysosomal enzymes palmitoyl protein thioesterase 1 (CLN1) (Vesa *et al.* 1995), TPP-I (CLN2) (Sleat *et al.* 1997), and cathepsin D (Tynnela *et al.* 2000), and three membrane proteins of unknown function [CLN3 (International Batten Disease Consortium 1995), CLN5 (Savukoski *et al.* 1998), and CLN8 (Ranta *et al.* 1999)]. Based on the substrate specificity of the above-mentioned three lysosomal enzymes and the lysosomal localization of the CLN3 protein (Jarvela *et al.* 1999), the NCLs seem to result from defects in a specific pathway through which membrane-associated hydrophobic proteins are normally degraded in lysosomes.

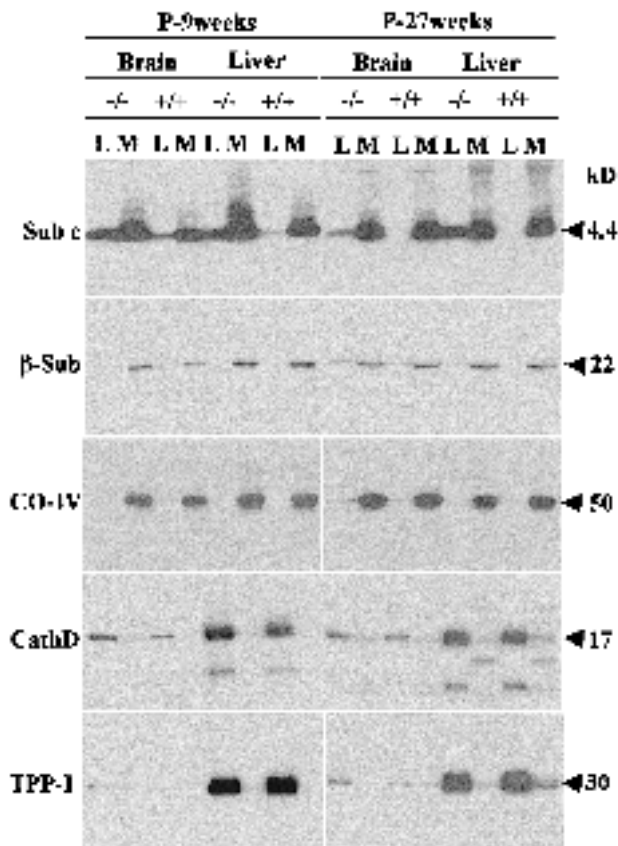


Figure 5 Lysosomal accumulation of subunit c in brain and liver of *Cln3*^{-/-} mice. Brains and livers were harvested and fractionated in Percoll density gradients into mitochondrial (M) and lysosomal (L) fractions as described in the methods section. The fractions were pooled separately and washed by repeated centrifugation. Ten micrograms of each protein sample was separated on 16.5% Tricine-SDS-PAGE for subunit c of ATP synthase (Sub c) and subunit IV of cytochrome oxidase (CO-IV), or on 12.5% SDS-PAGE for β-subunit of ATP synthase (β-sub), cathepsin D (CathD), and TPP-I. The gels were analysed by immunoblotting.

To investigate whether the neuronal degeneration in the *Cln3*^{-/-} mice had characteristics of NCL, we began a study by electron microscopy. As shown in Fig. 3, we confirmed the presence of lipofuscin-containing lysosomes in neurones and glia in the *Cln3*^{-/-} mice, although these deposits were not as conspicuous as those in the cathepsin D knockout mice (Koike *et al.* 2000). This may be related to the severity of NCL, since cathepsin D knockout mice die at postnatal day 26 ± 1 (Saftig *et al.* 1995) whereas some *Cln3*^{-/-} mice survive for longer. Subunit c of mitochondrial F1F0 ATPase, a very hydrophobic peptide, is known to be specifically accumulated in cells in many forms of NCL except in the infantile form (Hall *et al.* 1991; Kominami *et al.* 1992). Accordingly, we performed immunohistochemistry for subunit c in the brain and found that neuronal cell bodies in various regions of the brain in the *Cln3*^{-/-} mice were immunopositive (Fig. 4). This is consistent with the additional finding of cerebral atrophy in the aged *Cln3*^{-/-} mice, although drastic atrophy was predominant in the hippocampus. Western blotting of proteins after sub-cellular fractionation confirmed the accumulation of subunit c in the lysosomes in both the brain and liver. While small amounts of subunit c accumulation were found in neuronal cells, even in some types of lysosomal storage disorders other than NCL, there was no evidence of a significant lysosomal accumulation of subunit c in non-neuronal cells (Elleder *et al.* 1997). These data strongly suggested that the lysosomal accumulation of subunit c in the *Cln3*^{-/-} mice resulted from the dysfunction of a specific degradation pathway rather than a nonspecific one. This notion was also supported by the evidence that other mitochondrial proteins such as subunit β of ATP synthase and subunit IV of cytochrome oxidase were not accumulated in the lysosome in the *Cln3*^{-/-} mice (Fig. 5).

How could the CLC-3 deficiency impair the specific cellular degradation pathway? We confirmed that cathepsin D and TPP-I, enzymes with mutations that result in the accumulation of subunit c in lysosomes, were not impaired in maturation or protein abundance in lysosomes (Fig. 5). The molecular mechanism of accumulation of ceroid lipofuscin have not been clearly explained in most NCLs, especially in those whose responsible genes have been identified by reverse genetics (CLN3, CLN5, CLN8), such as those in this study. This study showed that the CLC-3 gene is important for the degradation of cellular proteins. Moreover, we were clearly able to show that the CLC-3 deficiency led to an elevation of pH within endosomes. As a chloride shunt pathway has been established to be necessary for efficient acidification within intracellular organelles, particularly in endosomes (Sonawane *et al.* 2002), CLC-3 could be

a channel responsible for this pathway in endosomes. Elevated lysosomal pH was recently reported in several forms of the NCLs (Holopainen *et al.* 2001), supporting the idea that the elevated pH in lysosomes may affect the catalytic activity of lysosomal enzymes, thus leading to the accumulation of ceroid-lipofuscin-like materials. However, the pattern of pH elevation in our NCL model, i.e. pH elevation not in the lysosome but in endosomes, could postulate that the elevated intravesicular pH directly influences not only the catalytic activity of lysosomal enzymes *in situ*, but also other biological processes such as the maturation of endosomes/autophagosomes, the binding of late endosomes to lysosomes, and the enhancement of the translocation or dislocation of proteins across the endosomes/autophagosomes to mature lysosomes. Thus, this study might shed new light on the pathogenesis of the NCLs. Similarly, Lonka *et al.* recently demonstrated that the CLN8 gene product is a protein not in lysosomes but in the endoplasmic reticulum. They speculated that CLN8 might act as a regulator of intracellular membrane transport (Lonka *et al.* 2000). At present, there is no unifying hypothesis which can explain the molecular mechanisms leading from defects of CLN proteins and CLC-3 to a relative uniform cellular phenotype. However, this study further supports the idea that pH homeostasis in intracellular organelles other than lysosomes may also be one of the major factors for proper proteolysis machinery.

In summary, we generated *Clcn3*^{-/-} mice by targeted gene disruption and found that the CLC-3 deficiency in mice led to elevated intraendosomal pH, influenced the cellular protein degradation cascade, and caused phenotypes similar to human NCL.

Experimental procedures

Clcn3 gene targeting

We isolated two overlapping λ phage clones from a 129/Sv strain mouse genomic library (Stratagene) using mouse *Clcn3* cDNA. An approximately 7.2-kb *Bam*HI fragment and a 1.9-kb *Xba*I fragment were isolated as the long arm and short arm, respectively, and used to construct a targeting vector in pLNTK. To generate the *Clcn3*^{-/-} mice, we electroporated and selected 129/Sv-derived E14 ES cells according to standard procedures. To screen homologous recombinant ES clones, we used a Southern blot analysis of *Eco*RI-digested DNA with the probe described in Fig. 1A. The expected sizes of the *Eco*RI bands for wild-type and mutant alleles are 5.8 kb and 3.7 kb, respectively. ES cells heterozygous for the targeted mutation were injected into C57BL/6 blastocysts to generate chimeras, and the resulting chimeras were then mated with C57BL/6 mice. The germ-line transmission of injected ES cells

was confirmed by the inheritance of agouti coat colour in the F1 animals, and all agouti offspring were tested for the presence of the mutated *Clcn3* allele by Southern blot analysis.

Protein analysis

Brain tissues were immediately frozen in liquid nitrogen and carefully broken down to a fine powder. Next, we suspended the powder in ice-cold 320 mM sucrose and homogenized the suspension with a glass-Teflon homogenizer (8 strokes, 1000 r.p.m.). The homogenate was twice centrifuged for 10 min at 47 000 g, and the resulting supernatant (S1) was combined and centrifuged for 40 min at 120 000 g to obtain S2 and P2. The S2 supernatant was further fractionated on a 700 mM sucrose cushion for 2 h at 260 000 g to obtain P3. We performed a Western analysis of each fraction using anti-rat CLC-3 antibody (1 : 200 dilution) (Alomone Laboratories, Jerusalem, Israel) and a Western Blue detection system (Promega).

Behavioural assessments

The hanging wire test (Sango *et al.* 1996) was performed by placing the mouse on the wire cage lid and turning the lid upside down. The investigator quantified the latency with which the mice fell from the wire lid. In the rotarod test, each mouse was given three consecutive trials at 5 r.p.m. In both tests a 60 s cut-off time was used for the standard test session. Locomotor activity was measured in the Multi-Digital 32-Port Counter System (Neuroscience Inc., Tokyo, Japan).

Histological analysis

Whole eyes, brains and internal viscera were fixed in 10% buffered neutral formalin. Routine processing, paraffin embedding and haematoxylin and eosin staining (H&E) were performed.

Electron microscopic analysis

Mice were fixed by cardiac perfusion with 2% paraformaldehyde-2% glutaraldehyde buffered with 0.1 M phosphate buffer (pH 7.2). Brains were cut into small pieces, and further immersed in the same fixative overnight at 4 °C. After washing thoroughly with the same buffer containing 7.5% sucrose, the samples were post-fixed with 1% OsO₄ with the same buffer containing 7.5% sucrose at 4 °C for 2 h. The brains were then block-stained with a 2% aqueous solution of uranyl acetate for 1 h, dehydrated with a series of ethanol, and embedded in Epon 812. Silver sections were cut with an ultramicrotome, stained with lead citrate and uranyl acetate, and observed with a Hitachi H-7100 electron microscope.

Immunohistochemistry

Mouse brains were perfused with 4% paraformaldehyde/PBS, immersed overnight, and snap-frozen in OCT compound in liquid nitrogen. Cryostat sections were prepared and fixed again in 4% paraformaldehyde/PBS for 15 min at room temperature. After

three washes with Tris-buffered saline with 1 mM calcium chloride (TBS-Ca), the sections were immersed in cold methanol for 10 min at -20°C , and nonspecific binding was blocked in 5% skimmed milk in TBS-Ca for 30 min at room temperature. Anti-F1F0 ATPase subunit c antibody diluted at 1 : 200 in 10% sheep serum in TBS-Ca was applied to each section and incubated overnight. After one wash with TBS-Ca, we applied Cy3-conjugated secondary antibody (Sigma) in 5% skimmed milk in TBS-Ca and incubated for 1 h at room temperature. Immunofluorescence was examined with an LSM-510 laser-scanning microscope (Carl Zeiss). A Vectastain ABC kit (Vector Laboratories, Burlingame, CA) was also used for staining subunit c in the paraffin sections.

Percoll density fractionation of brain and liver

Brains and livers were fractionated in Percoll density gradients into mitochondrial and lysosomal fractions as previously described (Ohshita & Kido 1995; Ohshita & Hiroi 1998). Equal amounts of proteins from control and *Clcn3*^{-/-} mice were separated on 16.5% Tricine-SDS-PAGE for subunit c of ATP synthase and subunit IV of cytochrome oxidase, or on 12.5% SDS-PAGE for β -subunit of ATP synthase, cathepsin D, and tripeptidylpeptidase I (TPP-I). The gels were analysed by immunoblotting.

Fluorescence pH measurement of liver endosomes

Endosomal pH measurement was performed as previously described (Van Dyke 1993). Briefly, after an intraperitoneal injection of 10 mg 70 000 molecular weight FITC-dextran, the livers were homogenated and centrifuged at 1000 g for 10 min to remove nuclei and unbroken cells. The supernatant (S1) was removed and centrifuged at 10 000 g for 20 min, and then the supernatant (S2) was removed and centrifuged at 100 000 g for 60 min to obtain a microsomal pellet containing FITC-dextran-loaded endosomes (P3). P3 was suspended in a small volume of incubation medium (100 mM KCl/10 mM MgCl₂/20 mM HEPES-KOH, pH 7.0/1 mM ATP), and the fluorescence was measured in a Spectrafluor fluorescence spectrophotometer (Wako). The vesicle pH was determined from the ratio of fluorescence intensity at two excitation wavelengths (492 and 450 nm excitation, 535 nm emission). In the range of pH 5.0–7.0, the ratio of fluorescence intensity was linearly related to the pH (data not shown). The addition of Triton X-100 disrupted the vesicles and exposed the incubation medium (pH 5.0 and pH 7.0) to FITC-dextran, thereby providing the calibration line.

Acknowledgements

This research was supported by grants-in-aid for scientific research from the Ministry of Education, Culture, Sports, Science and Culture of Japan, and the Salt Science Research Foundation.

References

Dawson, G. & Cho, S. (2000) Batten's disease: Clues to neuronal protein catabolism in lysosomes. *J. Neurosci. Res.* **60**, 133–140.

- Elleder, M., Sokolova, J. & Hrebicek, M. (1997) Follow-up study of subunit c of mitochondrial ATP synthase (SCMAS) in Batten disease and in unrelated lysosomal disorders. *Acta Neuropathol. (Berl.)* **93**, 379–390.
- Ezaki, J., Tanida, I., Kanehagi, N. & Kominami, E. (1999) A lysosomal proteinase, the late infantile neuronal ceroid lipofuscinosis gene (CLN2) product, is essential for degradation of a hydrophobic protein, the subunit c of ATP synthase. *J. Neurochem.* **72**, 2573–2582.
- Fahlke, C., Yu, H.T., Beck, C.L., Rhodes, T.H. & George, A.L. Jr (1997) Pore forming segments in voltage-gated chloride channels. *Nature* **390**, 529–532.
- Goebel, H.H. (1995) The neuronal ceroid-lipofuscinoses. *J. Child. Neurol.* **10**, 424–437.
- Goebel, H.H. & Sharp, J.D. (1998) The neuronal ceroid-lipofuscinoses. Recent advances. *Brain Pathol.* **8**, 151–162.
- Günther, W., Luchow, A., Cluzeaud, F., Vandewalle, A. & Jentsch, T.J. (1998) CLC-5, the chloride channel mutated in Dent's disease, colocalizes with the proton pump in endocytotically active kidney cells. *Proc. Natl. Acad. Sci. USA* **95**, 8075–8080.
- Hall, N.A., Lake, B.D., Dewji, N.N. & Patrick, A.D. (1991) Lysosomal storage of subunit c of mitochondrial ATP synthase in Batten's disease (ceroid-lipofuscinosis). *Biochem. J.* **275**, 269–272.
- Holopainen, J.M., Saarikoski, J., Kinnunen, P.K.J. & Jarvela, I. (2001) Elevated lysosomal pH in neuronal ceroid lipofuscinoses (NCLs). *Eur. J. Biochem.* **268**, 5851–5856.
- International Batten Disease Consortium (1995) Isolation of a novel gene underlying Batten disease, CLN3. *Cell* **82**, 949–957.
- Jarvela, I., Sainio, M., Rantamaki, T., *et al.* (1999) Biosynthesis and intracellular targeting of the CLN3 protein defective in Batten's disease. *Hum. Mol. Genet.* **7**, 85–90.
- Kawasaki, M., Uchida, S. & Monkawa, T. (1994) Cloning and expression of a protein kinase C-regulated chloride channel abundantly expressed in rat brain neuronal cells. *Neuron* **12**, 597–604.
- Koch, M.C., Steinmeyer, K., Lorenz, C., *et al.* (1992) The skeletal muscle chloride channel in dominant and recessive human myotonia. *Science* **257**, 797–800.
- Koike, M., Nakanishi, H., Saftig, P., *et al.* (2000) Cathepsin D deficiency induces lysosomal storage with ceroid lipofuscin in mouse CNS neurons. *J. Neurosci.* **20**, 6898–6906.
- Kominami, E., Ezaki, J., Munro, D., Ishido, K., Ueno, T. & Wolfe, L.S. (1992) Specific storage of subunit c of mitochondrial ATP synthase in lysosomes of neuronal ceroid lipofuscinosis (Batten's disease). *J. Biochem.* **111**, 278–282.
- Lonka, L., Kyttala, A., Ranta, S., Jalanko, A. & Lehesjoki, A.E. (2000) The neuronal ceroid lipofuscinosis CLN8 membrane protein is a resident of the endoplasmic reticulum. *Hum. Mol. Genet.* **9**, 1691–1697.
- Matsumura, Y., Uchida, S., Kondo, Y., *et al.* (1999) Overt nephrogenic diabetes insipidus in mice lacking the CLC-K1 chloride channel. *Nature Genet.* **21**, 95–98.
- Ohshita, T. & Hiroi, Y. (1998) Degradation of serum albumin by rat liver and kidney lysosomes. *J. Nutr. Sci. Vitaminol.* **44**, 641–653.
- Ohshita, T. & Kido, H. (1995) Simple preparation of rat brain lysosomes and their proteolytic properties. *Anal. Biochem.* **230**, 41–47.

- Piwon, N., Günther, W., Schwake, M., Bösl, M.R. & Jentsch, T.J. (2000) CLC-5 Cl⁻ channel disruption impairs endocytosis in a mouse model for Dent's disease. *Nature* **408**, 369–373.
- Ranta, S., Zhang, Y., Ross, B., *et al.* (1999) The neuronal ceroid lipofusinoses in human EPMR and mnd mutant mice are associated with mutations in CLN8. *Nature Genet.* **23**, 233–236.
- Saftig, P., Hetman, M., Schmahl, W., *et al.* (1995) Mice deficient for the lysosomal proteinase cathepsin D exhibit progressive atrophy of the intestinal mucosa and profound destruction of lymphoid cells. *EMBO J.* **14**, 3599–3608.
- Sakamoto, H., Sado, Y., Naito, I., *et al.* (1999) Cellular and subcellular immunolocalization of CLC-5 channel in mouse kidney: colocalization with H⁺-ATPase. *Am. J. Physiol.* **277**, F957–F965.
- Sango, K., McDonald, M.P., Crawley, J.N., *et al.* (1996) Mice lacking both subunits of lysosomal beta-hexosaminidase display gangliosidosis and mucopolysaccharidosis. *Nature Genet.* **14**, 348–352.
- Savukoski, M., Klockars, T., Holmberg, V., Santavuori, P., Lander, E.S. & Peltonen, L. (1998) CLN5, a novel gene encoding a putative transmembrane protein mutated in Finnish variant late infantile neuronal ceroid lipofuscinosis. *Nature Genet.* **19**, 286–288.
- Schmieder, S., Lindenthal, S. & Ehrenfeld, J. (2001) Tissue-specific N-glycosylation of the CLC-3 chloride channel. *Biochem. Biophys. Res. Commun.* **286**, 635–640.
- Simon, D.B., Bindra, R.S., Mansfield, T.A., *et al.* (1997) Mutations in the chloride channel gene, *CLCNKB*, cause Bartter's syndrome type III. *Nature Genet.* **17**, 171–178.
- Sleat, D.E., Donnelly, R.J., Lackland, H., *et al.* (1997) Association of mutations in a lysosomal protein with classic late-infantile neuronal ceroid lipofuscinosis. *Science* **277**, 1802–1805.
- Sonawane, N.D., Thiagarajah, J.R. & Verkman, A.S. (2002) Chloride concentration in endosomes measured using a ratioable fluorescent Cl⁻ indicator: Evidence for Cl⁻ accumulation during acidification. *J. Biol. Chem.* **277**, 5506–5513.
- Stobrawa, S.M., Breiderhoff, T., Takamori, S., *et al.* (2001) Disruption of CLC-3, a chloride channel expressed on synaptic vesicles, leads to a loss of the hippocampus. *Neuron* **29**, 185–196.
- Tyynela, J., Sohar, I., Sleat, D.E., *et al.* (2000) A mutation in the ovine cathepsin D gene causes a congenital lysosomal storage disease with profound neurodegeneration. *EMBO J.* **19**, 2786–2792.
- Van Dyke, R.W. (1993) Acidification of rat liver lysosomes: quantitation and comparison with endosomes. *Am. J. Physiol.* **265** (*Cell Physiol.* **34**), C901–C917.
- Vesa, J., Hellsten, E., Verkruyse, L.A., *et al.* (1995) Mutations in the palmitoyl protein thioesterase gene causing infantile neuronal ceroid lipofuscinosis. *Nature* **376**, 584–587.

Received: 20 February 2002

Accepted: 20 March 2002